Review: Sea Ice Albedo Bounded Data Assimilation and Its Impact on Modeling: A Regional Approach

This study investigates the impact of assimilating sea ice albedo (SIAL) on Arctic sea ice prediction using a series of perfect model experiments. The work is well-structured and addresses a relevant topic in data assimilation using the Quantile Conserving Ensemble Filtering Framework (QCEFF). The objective to evaluate the impact of SIAL assimilation on sea ice forecasts is clearly stated. The authors selected four diverse Arctic regions and use Icepack model for the assimilation with spin-up period (2000-2010) and experimental timeframe (2011-2015). The manuscript presents interesting results, particularly regarding the complementary benefits of multi-parameter assimilation. Several aspects of the experimental design and presentation could be clarified to strengthen the manuscript.

Thank you for sharing your overall favorable assessment.

Specific comments

1. Ensemble generation

The authors mentioned how to construct the ensemble but only in the abstract and L74 without details. It would be valuable to know the details on the ensemble generation, and elaborate in the Method section.

The authors appreciate this comment. The following section has been added to reflect this:

"To construct the ensemble, we employed the *Icepack* single-column sea ice model, configured to represent five Arctic regions of interest (Barents Sea, Coastal Canada, Siberian–Chukchi Seas, and the Central Arctic). Our ensemble was generated solely by perturbing external atmospheric forcing fields, following Appendix A of Wieringa and Bitz (in press), which ensures that perturbations retain realistic spatiotemporal coherence between atmospheric variables. In practice, this is achieved by perturbing the left singular vectors of the covariance matrix of the atmospheric state, such that the resulting ensemble members remain statistically consistent with the reference forcing fields.

Each ensemble member was initialized from a multi-year spin-up (2000–2010) to reduce sensitivity to initial conditions. Thirty ensemble members were produced for each experiment. For every member, a unique namelist file was created by perturbing selected atmospheric forcing fields (temperature, specific humidity, zonal and meridional wind, short- and longwave fluxes, and precipitation) using JRA-55-do reanalysis data. The ocean forcing remained identical across the ensemble. Specifically, the ocean component was represented by a slab ocean, with initial conditions extracted from the ocean output of a fully coupled historical CESM2 simulation. All ensemble members shared this common ocean forcing, ensuring that ensemble spread arose primarily from atmospheric forcing perturbations.

All members were integrated forward for the spin-up period using consistent external boundary conditions, after which restart files were generated at the end of 2010. These restart states served as the initial conditions for the assimilation experiments. Model output was collated across ensemble members, resampled to daily means, and combined into a single dataset with ensemble dimension. Ensemble mean and spread were calculated and stored in separate NetCDF files for subsequent analysis."

Note: The ocean initial conditions originate from a fully coupled CESM2 piControl simulation, corresponding to the B compset initialized in 1850 with the CAM6-WACM atmosphere. The prescribed ocean heat-flux forcing (qflux) is not taken directly from a single coupled simulation output, but is computed from climatological output of a fully coupled Ocean General Circulation Model (OGCM) following the methodology of Bitz et al. (2012). The resulting forcing file used here is pop_frc.b.e21.BW1850.f09_g17.CMIP6-piControl.001.190514.nc, previously archived on Derecho/Cheyenne (path may have changed over time). No additional appendix is provided, as this qflux forcing is applied directly at the model grid points used in this study.

2. Observation uncertainty

The assumptions for observation uncertainty are highly consequential for the DA results (Line ~170). The chosen setup—a parabolic distribution for SIC, 10% for SIT, and zero uncertainty at the bounds (0% and 100% SIC, 0m SIT)—is a common simplification but has significant implications. Setting uncertainty to zero forces the model to exactly match the observation at these bounds. This can lead to overconfidence and an artificial reduction in ensemble spread, potentially skewing the results. The authors could clarify this choice in the Methods or Discussion section. A strong recommendation for future work would be to adopt a more realistic uncertainty that avoids zero uncertainty, for instance, by specifying a minimum uncertainty floor (e.g., 1-2%) for SIC at 0% and 100%.

The authors agree that a more realistic uncertainty floor should be implemented to avoid zero uncertainty. In the initial setup, a fail-safe minimum of 10^{-7} was employed to prevent DART from rejecting observations with zero uncertainty. However, as the reviewer correctly notes, such small values can artificially accelerate the collapse of ensemble spread and reduce realism.

To address this, we re-ran the experiments with revised observation uncertainty specifications: a minimum of 0.01 for SIC at its bounds (0 and 1) and a minimum of 0.02 for SIT at its lower bound (0 m). During testing, we also found that when SIC approaches ~0, Icepack automatically assigns aggregate SIAL a value of 0 to represent open ocean. To ensure consistency, we therefore introduced a minimum uncertainty of 0.01 for SIAL as well. These revisions provide a more realistic treatment of observation error at the boundaries, preventing overconfidence while maintaining numerical stability in DART.

Implementing these corrections led to notable changes in our results. Figures 4–7 and the accompanying text have been updated accordingly. The key outcome is that all assimilation experiments performed better under the revised uncertainty scheme, as it prevented the collapse of model spread. Assimilating all variables together still produced the best results, and Figure 6 has been updated to reflect the advantages of multi-variate assimilation over SIC-only and/or SIT-only assimilation. Thus, while the overall conclusions of the study remain unchanged, the individual significance tests between assimilation experiments differ slightly under the more realistic uncertainty floor.

3. Interpretation of SIAL vs. SIC assimilation results

The central conclusion that SIAL assimilation outperforms SIC assimilation under low uncertainty is compelling. However, this advantage may be partially confounded by the differential uncertainty settings applied to each variable. SIAL's assigned uncertainty is likely low (though not explicitly stated in the provided text), while SIC's uncertainty is structurally defined by a parabola, which is higher everywhere except the bounds. A fairer comparison would require testing SIC assimilation under similarly low uncertainty assumptions. The authors may state this potential confounding factor in the discussion (e.g., around Line 306).

We thank the reviewer for this thoughtful comment. We acknowledge that the differing uncertainty formulations for SIAL and SIC may influence the comparison between assimilation experiments. Our choice of uncertainty settings was guided by previous studies (e.g., Karellson et al., 2024 for SIAL; Wieringa et al., 2024 for SIC and SIT), which reflect the distinct observational retrieval methods underlying these variables and their associated uncertainties. Specifically, SIAL retrievals are based on radiative transfer, requiring knowledge of reflected shortwave radiative fluxes at the top of the atmosphere, whereas SIC retrievals rely on passive microwave signals that exploit the emissivity contrast between open ocean and sea ice. Because these retrieval techniques are fundamentally different, it would not be physically consistent to impose identical uncertainty structures for both variables.

That said, we agree with the reviewer that further work is needed to systematically assess the role of uncertainty assumptions in data assimilation (DA) performance. In particular, future studies could explore the sensitivity of SIC assimilation to alternative (e.g., lower or more uniform) uncertainty settings to better isolate variable-dependent effects. For SIAL, we emphasize that uncertainty characterization remains an open research question, and we plan to investigate this aspect further. As the reviewer alluded, SIAL uncertainty is likely low, but the lack of spatially comprehensive in-situ measurements makes it difficult to validate the satellite footprint.

To address the potential impact of uncertainty distribution on our results, we re-ran the SIC-only assimilation experiments assuming a maximum SIC error of 5%, consistent with the “low” uncertainty setting used for SIAL. The results, shown in the figure below (excluded from the

manuscript for brevity), indicate minimal impact of the maximum SIC error on DA performance. The only notable improvement occurs in the Barents Sea for SIC RMSE, yet it remains insufficient to replicate the performance of the SIAL-only assimilation under low error. This supports our argument, discussed in the manuscript, that SIAL serves as a better predictor of melt onset—helping prevent filter divergence and reducing SIC RMSEs for thin, seasonal ice. Altogether, these findings suggest that our results are driven more by the intrinsic characteristics of the assimilated variable and its covariance with model state variables (e.g., *aicen* and *vicen*) than by the exact uncertainty distribution. As an aside, we note that the uncertainties used for SIC and SIT in our study are both likely lower than those observed in reality (e.g., SIC: Zhang et al., 2022; SIT: Fiedler et al., 2022).

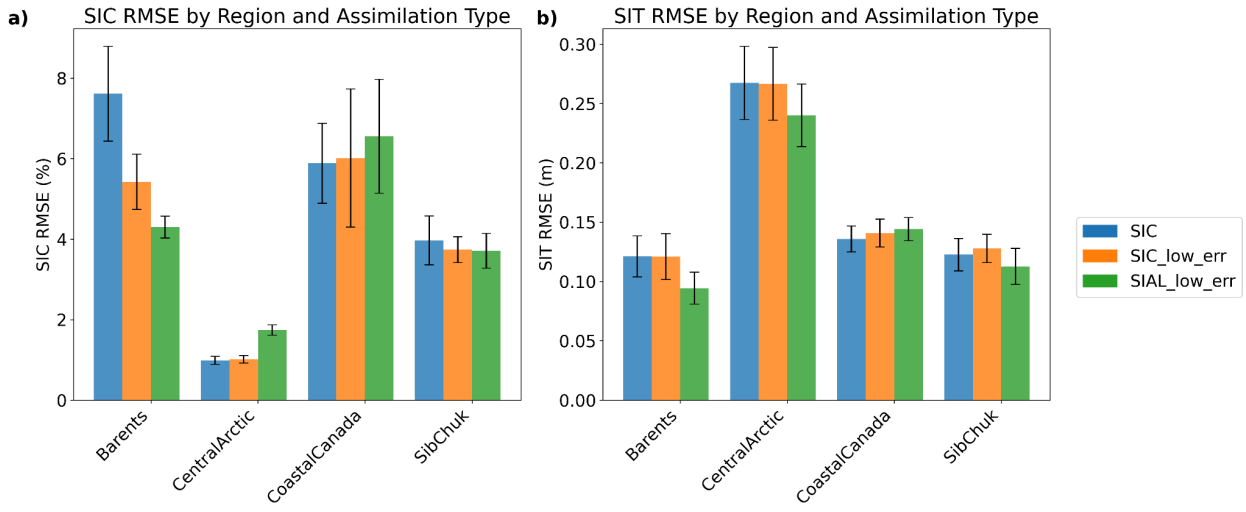

Figure A: Demonstration showing that varying the maximum SIC uncertainty (12.5% vs. 5%) has minimal influence on assimilation outcomes.

4. Multi-parameter assimilation

The finding that the simultaneous assimilation of SIC, SIT, and SIAL yields the best performance is a key result. The complementarity between these variables, as likely illustrated in Figure 4, is a highly valuable insight. This multi-parameter complementarity deserves to be highlighted and discussed in greater depth as a major takeaway of the study, perhaps exploring the physical reasons behind why the constraints provided by these variables are non-redundant.

The authors agree and thank the reviewer for this insightful comment. We have revised Figure 6 to emphasize the benefits of multivariate assimilation, focusing on the combined assimilation of SIC, SIT, and SIAL rather than individual comparisons of SIC-only, SIT-only, and SIAL-only experiments. This updated figure highlights the consistent advantages of assimilating multiple parameters over single-variable approaches. Accordingly, we are revising the discussion and conclusions sections to center on multi-variate assimilation as a primary theme.

The likely physical explanation for this improvement lies in albedo's role in capturing the melt season. As temperatures rise, *Icepack* simulates melt pond formation and decreasing snow cover, both of which provide additional information on ice melt processes. While SIC and ice volume may not yet show a steady decline, the reduction in snow and exposure of darker underlying surfaces allow albedo assimilation to precondition the ice to melt under higher model spread, despite albedo not being a prognostic variable. Consequently, when combined with SIC and SIT assimilation, the ensemble framework produces more physically consistent updates (particularly for SIC increments) leading to improved overall assimilation performance.

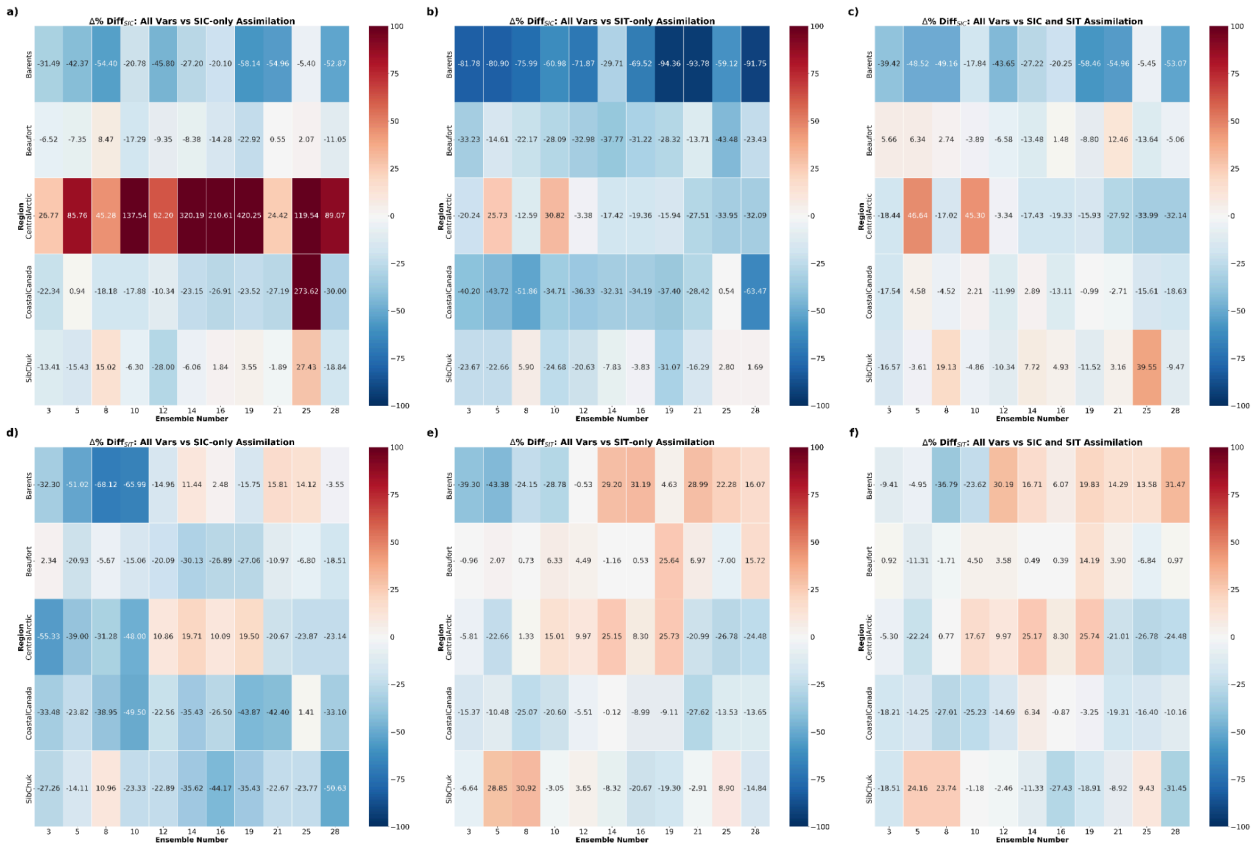

Figure B: Revised version of Paper Figure 6, emphasizing the benefits of multivariate assimilation when using the *level* melt pond scheme, except for Coastal Canada and the Siberian Chukchi Sea which use the *topographic* melt pond scheme (see below for more details on why we add this specification).

5. Region-specific behavior of albedo (Section 4.3)

The identified unique albedo evolution for category `n=1` ice in the Chukchi Sea is interesting. Is there any reason for that? the formation of melt ponds? Why is it pronounced in this region and not in others?

We have delved deeply into this particular result, after developing several theories as to why SIAL assimilation in the Siberian-Chukchi Sea produced worse performance when error is unconstrained. First, we looked into the development of thinner ice in category $n = 1$ as suggested by the reviewer. Because *Icepack* only represents a single discrete point, the user must specify what to import when the ice undergoes closing. The available options are to import open water or uniform ice. For this region, we opted to import open water into the grid cell since this region is assumed to be near the sea ice edge most of the year. Hence, under closing, when existing ice is rafted or ridged, leads form. Upon refreezing thin, snow-free ice forms and populates category $n = 1$.

This behavior contrasts with that in the Coastal Canada region, which experiences a similar seasonal SIC cycle (as shown in Figure 2 of the main manuscript). There, we elected the uniform ice option, which imports ice with the same conditions (ice thickness distribution, snow depth, etc.) as are present in the grid cell as rafting and ridging occur. For clarity, a categorical comparison illustrating this behavior is provided in Figure C.

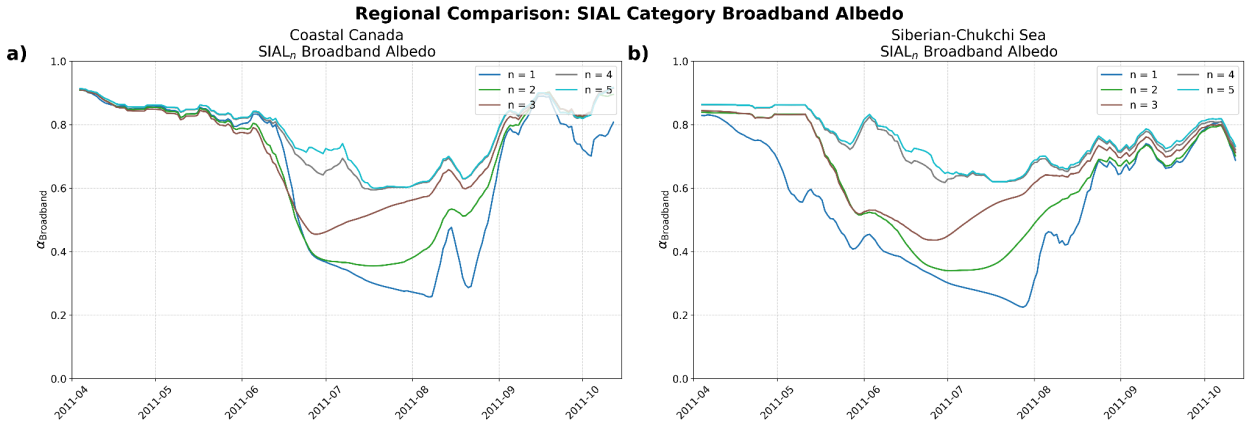

Figure C: The SIAL cycle per category n between two regional ice coverage locations where Coastal Canada experienced uniform ice fluxing and Siberian–Chukchi Sea experienced open water fluxing.

In a fully dynamical ice configuration, the imported ice would likely lie between the open-water and uniform-ice closing cases. While this distinction may influence results to some extent elsewhere, it is unlikely to have a major effect, particularly at the satellite pixel scale. The chosen import scheme helps explain the degraded performance of SIAL assimilation relative to the free run in the Siberian–Chukchi Sea.

Because SIAL assimilation aggregates albedo information across categories, it introduces negative SIC innovations earlier in the melt season, leading to premature melt relative to the truth (as shown in the accompanying Figures D & E, excluded from the paper for brevity). From Figure 7, we see that assimilating SIAL by category avoids this early negative innovation. If

category-specific assimilation were implemented, the innovations would reveal that only SIAL in category $n = 1$ decreases substantially early in the Siberian–Chukchi Sea melt season, indicating that ice in other categories remains largely unaffected by melt. This information would constrain the assimilation to slow the rate of sea ice loss. In contrast, large negative aggregate innovations push SIAL states beyond the observational range, producing a model evolution that diverges from the truth and melts too early (Fig. E).

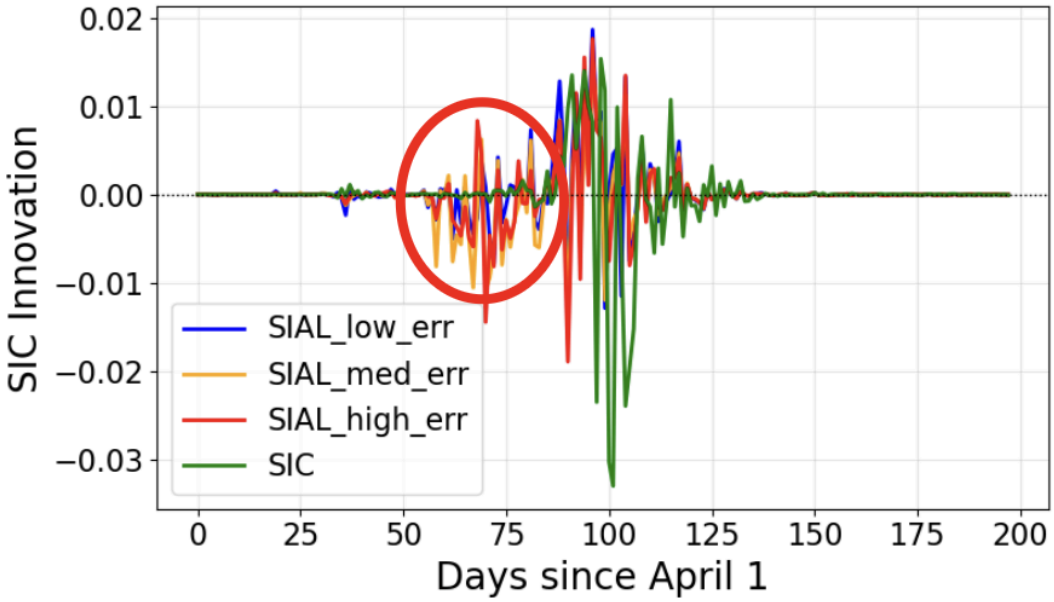

Figure D: Early melt-season negative innovations from SIAL assimilation in the Siberian–Chukchi Sea.

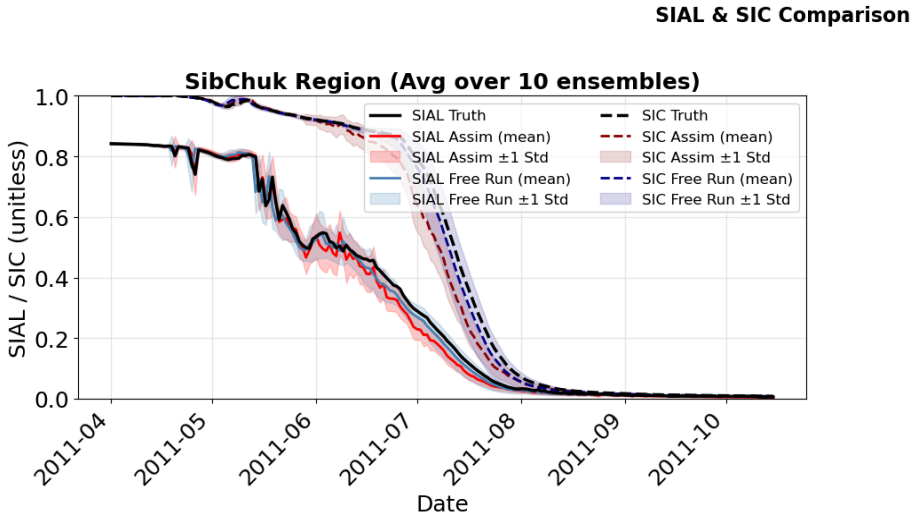

Figure E: New model state in the Siberian–Chukchi Sea showing reduced ice coverage—less than in the free run—resulting from negative innovations.

Since submitting the paper, **the authors have identified a more likely source of the discrepancy contributing to the higher-than–free-run error for SIAL assimilation in the Siberian–Chukchi Sea and the near-baseline performance in Coastal Canada.** The melt pond fraction in the version of *Icepack* (1.4.1) used for this study is unrealistically high compared to observations, which suggest a maximum melt pond coverage of roughly 50% during the melt season (Niehaus et al., 2024). As shown in Figure F below, the simulated melt pond fraction approaches unity during the melt season in Coastal Canada and the Siberian–Chukchi Seas, leading to erroneous sea ice updates. This unrealistic melt pond behavior is likely responsible for the early negative SIC innovations and associated negative updates discussed above. Below, we diagnose methods to assess the impact of melt pond schemes on our results, and suggest differential melt pond schemes for different regions.

Since this work was submitted, efforts have been underway to improve the melt pond parameterization in *Icepack*, with new schemes currently in development and submission. The authors have added this discussion to clarify why SIAL assimilation in the Coastal Canada and Siberian–Chukchi regions may not perform as well as initially anticipated within the 'Results' and 'Discussion' Sections. Notably, melt pond evolution appears more realistic in the Barents region (reaching only ~30% coverage before completely ice-free conditions), which likely explains why SIAL assimilation under the level melt pond scheme there produces markedly improved results.

To further investigate the source of this unrealistic melt pond evolution, the authors examined the melt pond scheme used in these experiments—the "level pond" scheme (see Icepack Documentation Section 2.7.2.2). In this scheme, ponds form and are evenly distributed across all level ice. Because closing rates are specified from the SHEBA campaign (1998), which took place in perennial sea ice conditions, they are likely biased low for seasonal ice locations (e.g., Coastal Canada and the Siberian–Chukchi Seas). As a result, the ice is too level (~95–100%, not shown), allowing melt ponds to quickly spread across the surface. During the melt season, this causes the simulated albedo to drop unrealistically, as if the surface were largely melt pond water. This mechanism likely explains the premature melt and excessive albedo reduction observed in the SIAL assimilation runs—a model representation error rather than a physical response. The authors therefore do not expect these early-melt artifacts to occur outside this idealized *Icepack* configuration. Incorporating full CICE, with its dynamic treatment of rafting and ridging, would likely yield a more realistic melt pond distribution in the early melt season and mitigate this issue.

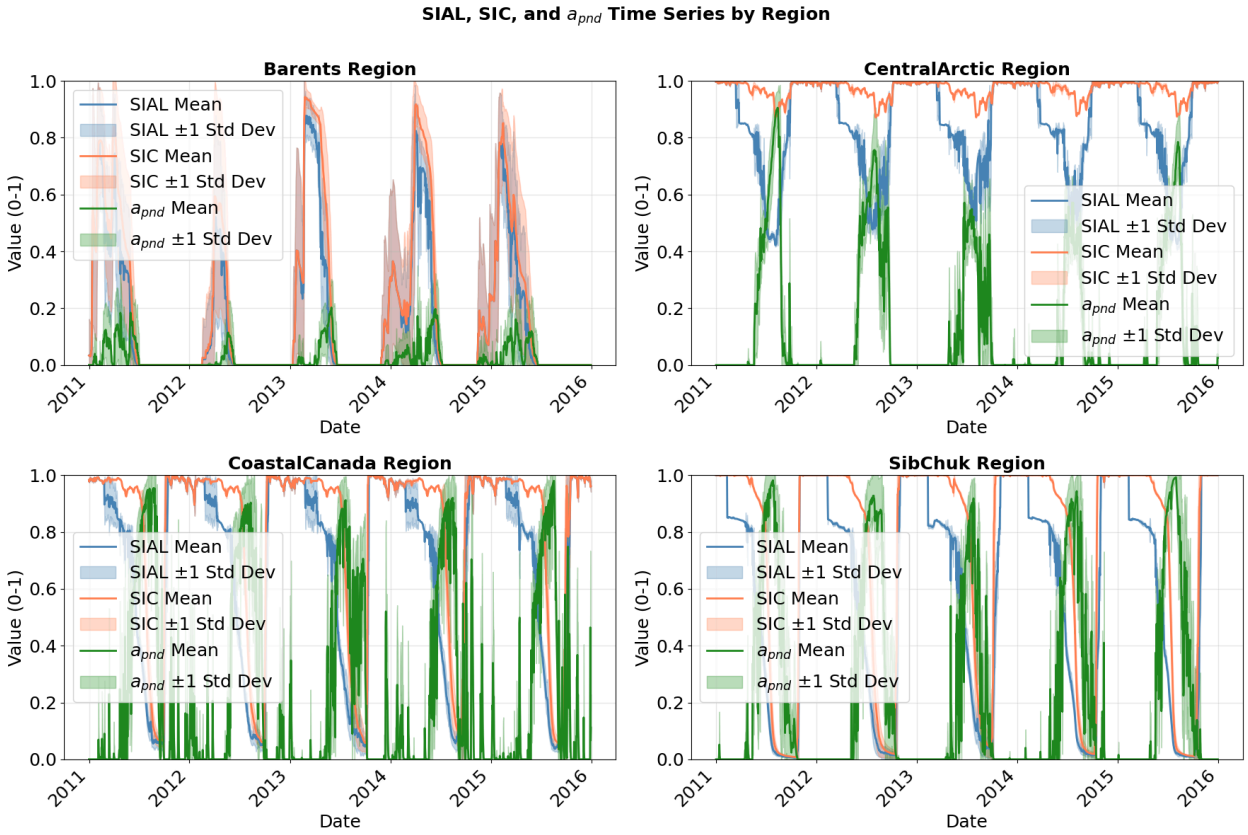

Figure E: Erroneous melt pond behavior in the Coastal Canada and Siberian–Chukchi regions. Although melt pond depths are modest, the ponded areas appear excessive—unlike in the Barents Sea—leading to substantial negative SIC innovations and a new model state with reduced ice coverage.

Fortunately, the version of *Icepack* that we used for this study did have the ability to use the "topographic" melt pond scheme. This melt pond scheme is generally not recommended for general model use because it assumes an empirical form of melt ponds that does not transfer well to future climates based on conversations with Elizabeth Hunke, a main developer of the Community Ice CodE (CICE), which encompasses *Icepack*. For the purpose of our experiments, however, we reran all cases under the topographic melt pond scheme. Doing so removed the unrealistic higher-than-free run SIC RMSEs within the Siberian Chukchi Sea, and near-baseline performance in Coastal Canada. We ran a comparison of SIC RMSE reductions between both melt pond schemes to determine which scheme we should use by region in our results. The experiment revealed that we must use the level melt pond scheme for more accurate SIC representation in all regions except Coastal Canada and the Siberian-Chukchi Sea regions, where the topographic melt pond scheme statistically outperforms the level melt pond scheme for SIC representation across all assimilation configurations. This is given in Figure F below.

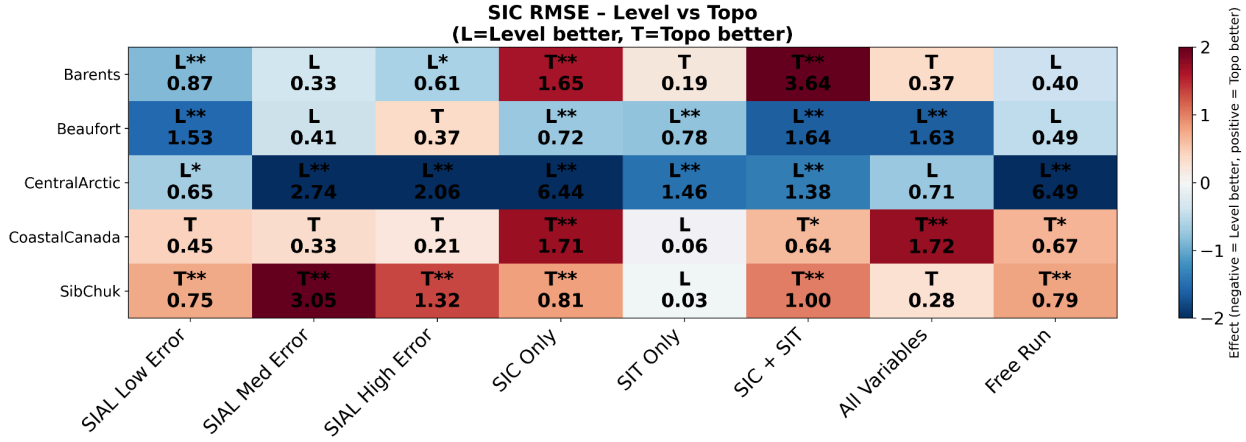

Figure F: Comparison of SIC RMSE for the topographic and level melt pond schemes. "T" indicates that the topographic scheme performed better, and "L" indicates that the level pond scheme performed better. The asterisk indicates significance; where "*" indicates $p < 0.1$ and "**" indicates $p < 0.05$.

Thus, for Coastal Canada and the Siberian-Chukchi Sea we opted to use the topographic melt pond scheme to reflect a more realistic melt pond fraction (and therefore albedo) for this location, keeping the more physical level melt pond scheme for the remaining regions. Such a more realistic melt pond fraction then led to improved assimilation performance across the board. Updated paper figures (Figs. B above and H below) are included below for emphasis of this change.

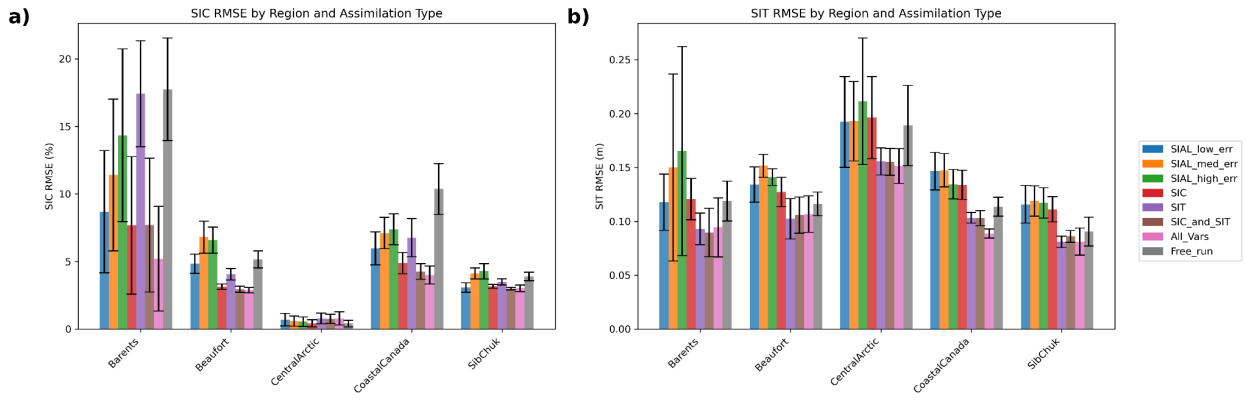

Figure G. Updated version of Figure 4 from the preprint, reflecting the addition of the Beaufort Sea region (as requested by Reviewer 3) and the switch to the topographic melt pond scheme for Coastal Canada and the Siberian–Chukchi Sea.

To further confirm that the topographic melt pond scheme better matched observed albedo observations in Coastal Canada and the Siberian Chukchi Sea, we compared our simulated experiments to satellite observations to illustrate an improved representation of ice-covered

albedo. Although the model contained a large negative bias in observed SIC, we compared the albedo *only* over ice-covered regions from satellite observations (using bilinear interpolation) with simulated albedos. Within the Siberian-Chukchi Seas, we see improved representation of albedo over ice-covered portions of the observed grid cell when using the topographic melt pond scheme (Figs. H and I). Thus, the authors feel confident in the chosen melt pond scheme for Coastal Canada and the Siberian-Chukchi Sea, despite being advised to not generally use this melt pond scheme in practice. We hypothesize that using full CICE (which includes a 2D dynamical representation of sea ice) would mitigate this degradation associated with the level melt-pond scheme by providing a more realistic dynamical evolution, thereby preventing near-unity coverage of level sea ice and the overrepresentation of melt-pond fraction.

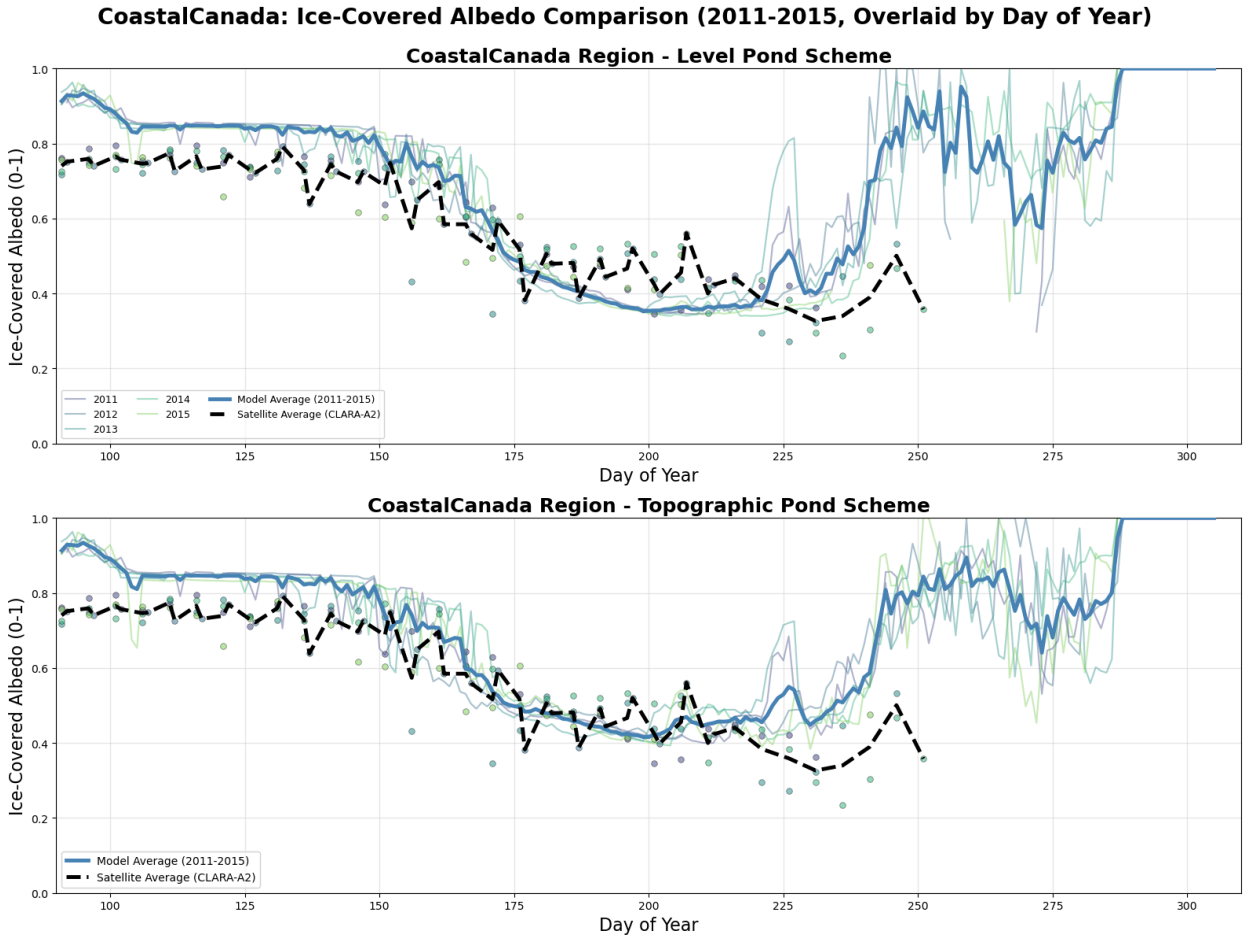

Figure H: SIAL representation averaged seasonally (April 1 - October 15) over the free run period (2011-2015) for the model *Icepack* (blue line) and the satellite data (CLARA-A3 and NSIDC CDR) for Coastal Canada.

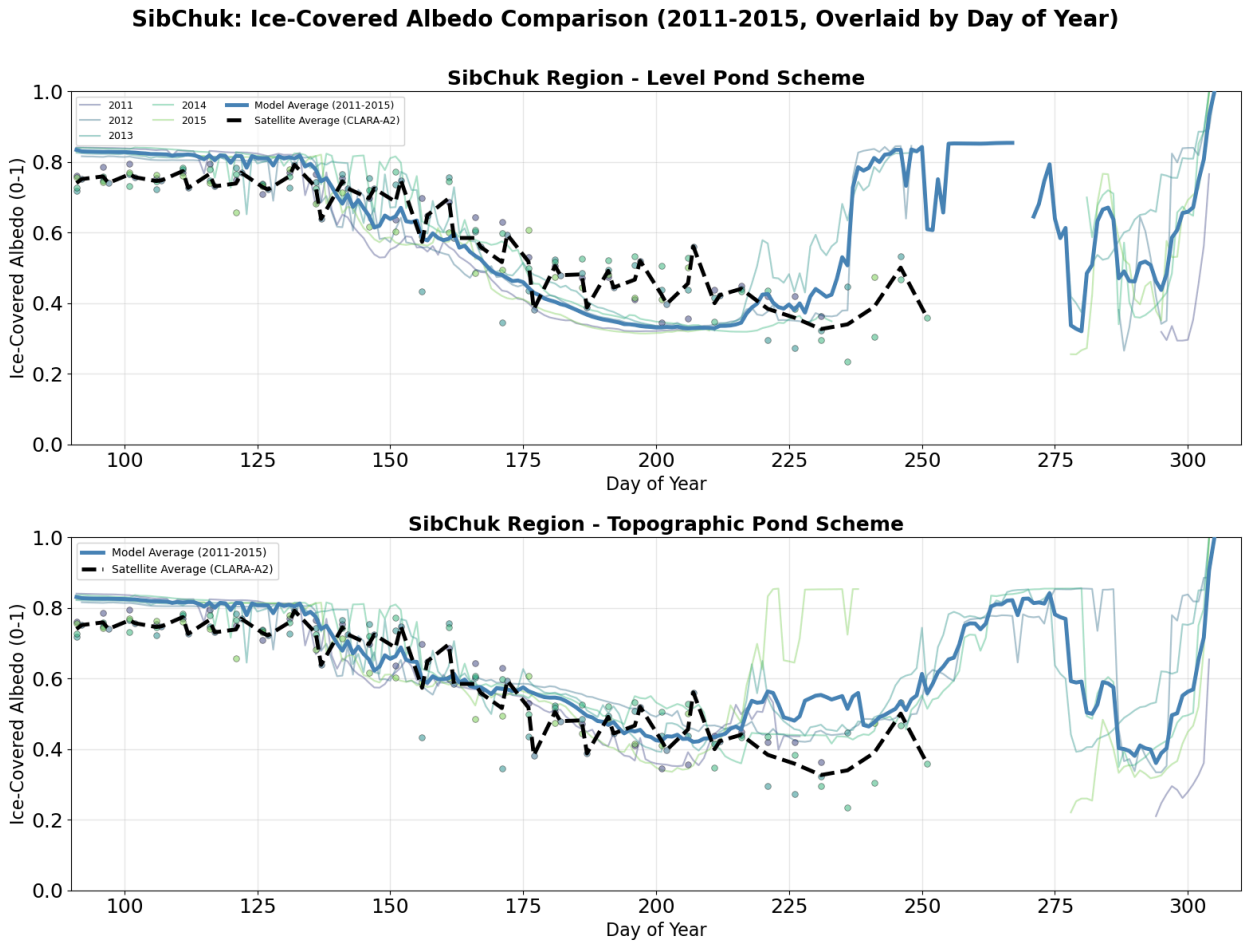

Figure I: SIAL representation averaged seasonally (April 1 - October 15) over the free run period (2011-2015) for the model *Icepack* (blue line) and the satellite data (CLARA-A3 and NSIDC CDR) for the Siberian-Chukchi Sea.